

# Stress-Strain Relation of Confined Concrete under Dynamic Loading

S.Kono & F.Watanabe

Department of Architecture, Kyoto University, Kyoto, Japan

Akihiro Kajitani

Government of Fukuoka Prefecture, Fukuoka, Japan

**ABSTRACT:** A dynamic compression test was carried out on 126 cylinder specimens, which has 75 mm in diameter and 150 mm in height with or without confining spirals, in order to study strain rate effects on the stress-strain relation of confined concrete. Test variables were strain rate (static to 0.1/s), original compressive concrete strength (30 MPa to 54MPa), amount of confining spiral (unconfined to 2.0% in volume ratio), and its yield strength (300 MPa and 850 MPa). It was found that the unconfined concrete had a strong strain rate sensitivity with respect to the peak stress and peak strain but the sensitivity decreased as the confining transverse stress increased. The enhanced peak stress increased linearly with the confining transverse stress when specimens had a same strain rate.

## 1 INTRODUCTION

### 1.1 Background

A great number of studies on confined concrete have been conducted for decades and fundamental knowledge about the confined concrete under static loading has been accumulated. Desayi et al. (1978), Park and Leslie (1977), Watanabe et al. (1980), Mander et al. (1988), Fafitis and Shah (1985) studied effects of shape, amount, and yield strength of confining reinforcement and the original compressive strength of concrete on the axial stress-strain relation of confined concrete under static loading. They proposed models to predict the stress-strain relation but those models do not always agree with other experimental results.

Although fundamental knowledge have been accumulated on stress-strain relation of confined concrete under the static loading, variations of those properties under dynamic loading have not been clarified yet. If the properties of concrete vary with the strain rate, the resisting mechanisms of reinforced concrete members may also differ from those under static loading. As a result, experimental results under static loading may not be directly applied to predict behaviors under dynamic loading. For example, when a member is designed based on the experimental results under static loading, the unexpected shear failure may result if the dynamic effect increases the flexural capacity with keeping shear capacity constant. Strain rate effects on the axial stress-strain relation have been studied by Ahmad and Shah (1985), Dilger et al. (1984), Soroushian et al. (1986a, 1986b), and Mander et al. (1988a, 1988b) but they do not agree on factors which determine the stress-strain relation under dynamic loading. In addition, they do not necessarily

report a variation of confining pressure with the progress of axial strain and it is not clear if the variation of peak stress and peak strain resulted from strain rate effects or confining effects.

### 1.2 Objectives

A total of one hundred twenty-six cylinder specimens with 75 mm in diameter and 150 mm in height was tested and the change of axial strain, axial stress, and transverse strain was measured in order to study the strain rate effects on the compressive axial stress-strain relation of confined concrete. Four test variables in the experiment were the original concrete compressive strength, the amount and the yield strength of confining spiral, and the strain rate. Authors aim to predict a complete stress-strain relation of confined concrete under dynamic loading but the outline and the main findings of the experiment are reported in this paper. Two objectives in this paper are 1) to evaluate the effect of strain rate, original concrete compressive strength, amount and the yield strength of confining spiral on the peak stress, the peak strain, and the transverse stress at the peak, and 2) to observe the change of failure modes for specimens under different strain rates.

## 2. EXPERIMENTAL SETUP

Figure 1(a) shows dimensions of cylinder specimens. Each specimen has two steel tripods embedded at 35 mm from the top and the bottom faces in order to measure the relative axial displacement between these two locations. The tip of each pod has a hole so that a bolt to fix the measuring rig shown in Figure 1(b) can be fixed. In this paper, the average relative displacement between two

Table 1. Specimen designations, test variables, and test results.

Specimen		Number of tested specimens	Test variables				Test results					
Set	Series		Concrete compressive strength $f'_c$ (MPa)	Spiral		Planned Strain rate $\dot{\nu}$ (1/s)	Average strain rate (1/s)	Average peak stress (MPa)	Strain rate sensitivity of peak stress $D_f$	Average Peak strain (%)	Strain rate sensitivity of peak strain $D_s$	
				Nominal yield strength $f_y$ (MPa)	Volume ratio $\rho$ (%)							
30N0	30AN0	3	30.0	None	None	3.10E-05	3.10E-05	29.2	1.00	0.23	1.00	
	30BN0	3				1.17E-03	1.30E-03	31.6	1.08	0.22	0.94	
	30CN0	3				1.17E-02	1.69E-02	33.9	1.16	0.17	0.74	
	30DN0	2				1.34E-01	1.32E-01	38.9	1.33	0.28	1.20	
30H1	30AH1	2		0.88	850	3.50E-05	3.50E-05	36.0	1.00	1.92	1.00	
	30CH1	3				1.34E-02	1.44E-02	39.9	1.11	1.52	0.79	
30H2	30AH2	3		1.76	850	3.10E-05	3.10E-05	63.2	1.00	2.87	1.00	
	30BH2	3				2.01E-03	1.81E-03	62.6	0.99	3.11	1.08	
	30CH2	3				1.34E-02	1.37E-02	64.2	1.02	2.65	0.92	
	30DH2	3				1.34E-01	1.53E-01	66.6	1.06	2.57	0.89	
30L2	30AL2	3		1.76	300	3.50E-05	3.50E-05	41.1	1.00	1.42	1.00	
	30CL2	3				1.34E-02	1.48E-02	44.3	1.08	1.15	0.81	
32N0	32AN0	3		31.8	None	None	4.80E-05	4.94E-05	31.8	1.00	0.24	1.00
	32BN0	2					1.30E-03	1.67E-03	33.1	1.04	0.25	1.05
	32CN0	3					1.30E-02	2.61E-02	35.5	1.11	0.24	0.99
	32DN0	2					1.30E-01	1.48E-01	41.7	1.31	0.29	1.22
32H1	32AH1	2	0.90		850	4.80E-05	4.78E-05	44.0	1.00	2.03	1.00	
	32CH1	3				1.30E-03	1.34E-03	45.5	1.03	1.86	0.92	
	32AH1	3				1.30E-02	1.45E-02	45.4	1.03	1.64	0.81	
32H2	32CH1	3	1.81		850	1.30E-01	1.71E-01	47.7	1.09	1.30	0.64	
	32AH2	2				4.80E-05	4.85E-05	81.6	1.00	3.30	1.00	
	32BH2	2				1.30E-03	1.32E-03	78.7	0.96	3.17	0.96	
	32CH2	3				1.30E-02	1.37E-02	80.0	0.98	2.96	0.90	
32L1	32AL1	3	0.97		300	1.30E-01	1.47E-01	76.8	0.94	3.31	1.00	
	32CL1	3				3.50E-05	4.81E-05	38.3	1.00	0.81	1.00	
35N0	35AN0	3	35.0		None	None	1.34E-02	1.72E-02	40.9	1.07	0.70	0.86
	35BN0	4					3.10E-05	3.30E-05	35.4	1.00	0.21	1.00
	35CN0	3					1.17E-03	1.23E-03	39.7	1.12	0.17	0.82
	35DN0	2		1.18E-02			1.36E-02	44.7	1.26	0.19	0.93	
35H1	35AH1	2		0.88	850	1.34E-01	1.32E-01	46.9	1.32	0.25	1.21	
	35CH1	4				3.10E-05	3.10E-05	47.0	1.00	1.24	1.00	
35H2	35AH2	3		1.76	850	1.17E-02	1.55E-02	47.3	1.01	0.67	0.54	
	35BH2	3				3.10E-05	3.10E-05	72.7	1.00	1.55	1.00	
	35CH2	3				1.17E-03	1.19E-03	73.9	1.02	1.31	0.84	
	35DH2	2				1.17E-02	1.24E-02	74.3	1.02	1.48	0.96	
54N0	54AN0	5		54.8	None	None	1.34E-01	1.61E-01	76.2	1.05	1.33	0.86
	54BN0	3					4.80E-05	4.86E-05	54.8	1.00	0.29	1.00
	54CN0	3					1.30E-03	1.49E-03	55.3	1.01	0.25	0.87
	54DN0	3					1.30E-02	1.90E-02	59.9	1.09	0.30	1.04
54H1	54AH1	3			1.81	850	1.30E-01	1.32E-01	64.9	1.18	0.34	1.19
	54BH1	3					4.80E-05	4.78E-05	69.1	1.00	0.50	1.00
	54CH1	3	1.30E-03				1.47E-03	71.1	1.03	0.41	0.81	
	54DH1	3	1.30E-02				1.87E-02	80.1	1.16	0.35	0.69	
						1.30E-01	1.58E-01	85.1	1.23	0.44	0.88	

tripods were used to calculate the axial strain. In a pilot test, the strain computed from the three displacement gages agreed very well with the average strain obtained from three 60 mm long foil strain gages, which were attached on the concrete surface parallel to the displacement gages. Since strain gages cannot measure large strain expected

for highly confined specimens, displacement gages were chosen to measure the axial strain for all specimens. Figure 1(c) shows strain gage locations to measure the transverse strains: three gages on an unconfined cylinder surface and six or eight gages on spirals. The spirals had two types of spacing (20 mm or 40 mm) and two kinds

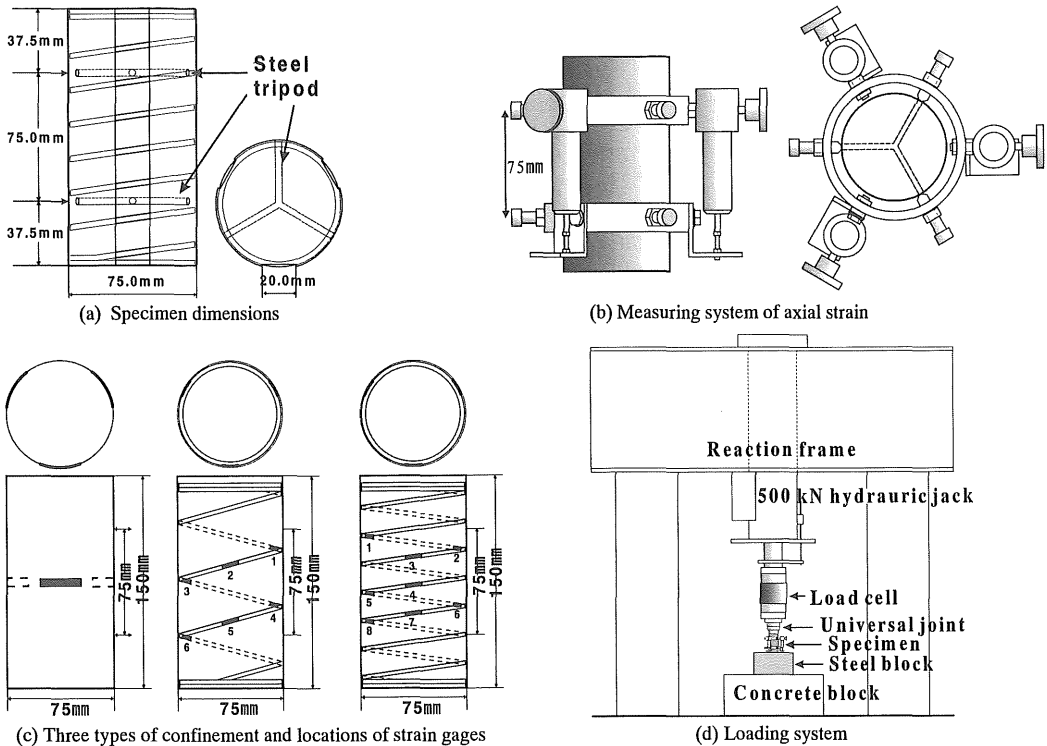


Figure 1. Specimen dimensions, measuring system, and loading system.

of yield strengths. The high strength spirals had a yield strength of 850 MPa with 2.9 mm diameter and the low strength spirals had a yield strength of 300 MPa with 3.0 mm diameter.

Cylinders were loaded concentrically with a servo hydraulic actuator with a 500 kN capacity as shown in Figure 1(d). The actuator used the relative displacement between two tripods as a feedback signal to achieve a desired strain rate.

Four kinds of test variables were employed as shown in Table 1. They are the original concrete strength ( $f'_c = 30 \text{ MPa}, 32 \text{ MPa}, 35 \text{ MPa}$  or  $54 \text{ MPa}$ ), the yield strength of confining spiral ( $f_y = 300 \text{ MPa}$  or  $850 \text{ MPa}$ ), the amount of confining spiral (volume ratio  $\rho = 0.0 \%$ ,  $0.9 \%$ , or  $1.8 \%$  in), and the strain rate ( $\nu =$  quasi-static,  $1.3\text{E-}3/\text{s}$ ,  $1.3\text{E-}2/\text{s}$ , or  $1.3\text{E-}1/\text{s}$ ). Volume ratio,  $\rho$ , was obtained by dividing the volume of spiral by the volume of core concrete where the volume of concrete core was based on the inner span of the spiral. Multiple specimens were tested for a combination of the test variables and a total number of specimens was one hundred twenty-six.

### 3. TEST RESULTS

#### 3.1 Failure modes

Figures 2(a) through (j) show selective photos of specimens after testing. Specimens generally contracted con-

centrically and failed in the central instrumented region. They have some vertical major and micro cracks as schematically shown in Figure 2(k). Some specimens failed with a diagonal failure plane as shown in Figure 2(l) or with a combination of Figures 2(k) and (l). Specimens with too much eccentric deformation or with failure too close to the top or bottom surface are not included in Table 1. Generally speaking, specimens did not show any specific failure mode particular for a certain combination of test variables. Mander et al. (1988b) reported that a strongly defined diagonal failure plane was characteristic of test units with comparatively low volumetric ratios of confining steel but this was not the case in this experiment.

#### 3.2 General shape of axial stress - strain curves

Figure 3 shows selective axial stress-strain relations averaged for specimens with a same combination of test variables. Multiple lines are placed in a same plot if they have a same combination of test variables except strain rates. The peak stress, the peak strain, and the energy dissipation increase as the confinement increases but the shapes of the curves in a same plot are similar. This change of the shape due to confinement at any strain rate seems to follow that under static loading and the effect of strain rate on the shape cannot be clearly seen in Figure 3.

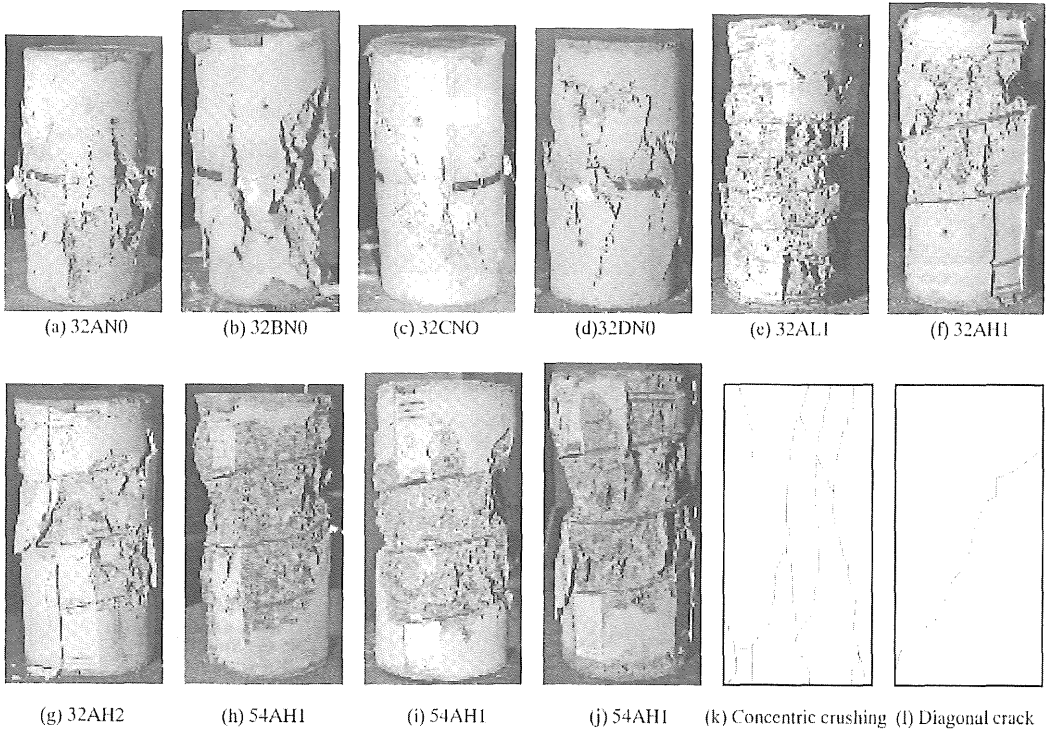


Figure 2. Selective specimens after testing and observed typical failure modes.

### 3.3 Strain rate sensitivity of peak stress and peak strain

Two steps can be taken in order to predict the axial stress-strain relation for confined concrete under dynamic load-

ing. First, the peak stress and peak strain are determined considering confining effects and strain rate effects. Second, based on the predicted peak stress and peak strain values from the first step and mechanical properties of unconfined concrete under static loading, the shape

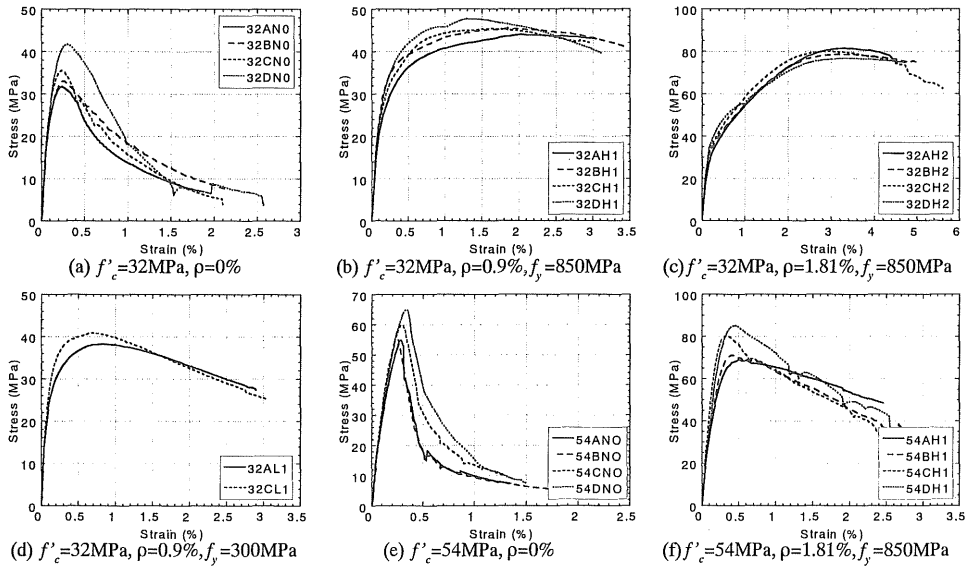
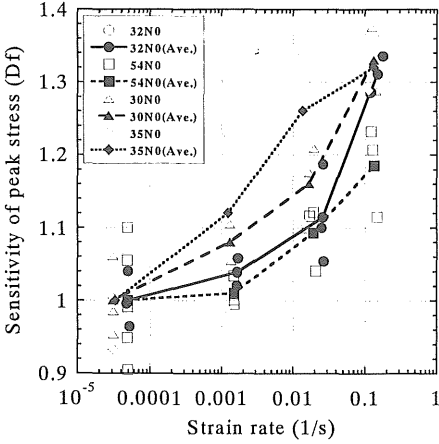
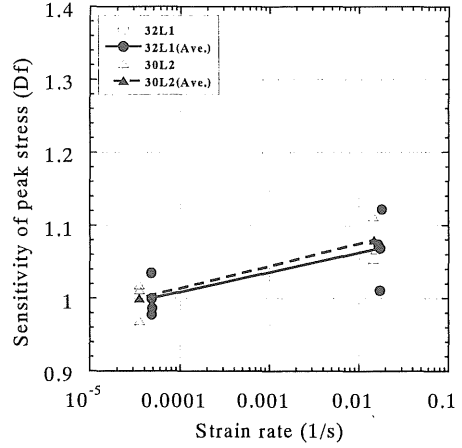
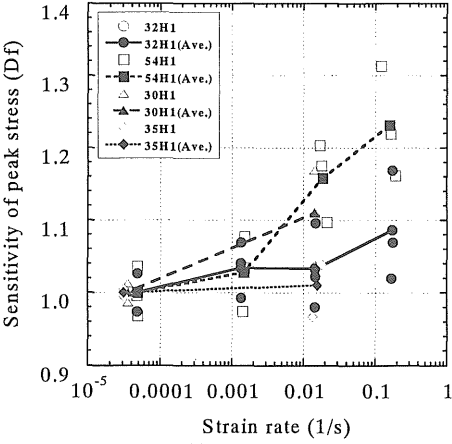
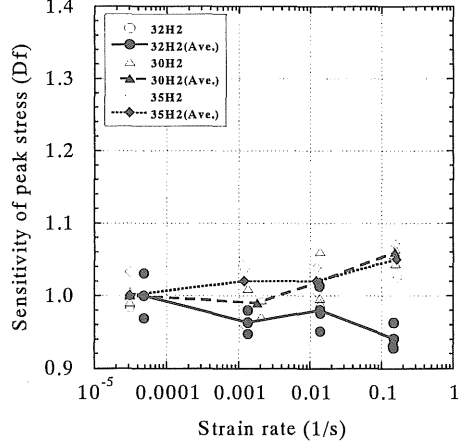


Figure 3. Average axial stress and Average strain relations for specimens with same combination of test variables.

(a)  $\rho=0\%$ (b)  $\rho=0.9\%, f_y=300\text{MPa}$ (c)  $\rho=0.9\%, f_y=850\text{MPa}$ (d)  $\rho=1.81\%, f_y=850\text{MPa}$ Figure 4. Strain rate sensitivity of peak stress,  $D_f$ 

$$D_f = \frac{f'_{cc}}{f'_c} \quad (1)$$

$$D_s = \frac{\varepsilon_{cc}}{\varepsilon_c} \quad (2)$$

where  $f'_{cc}$  and  $\varepsilon_{cc}$  are the peak stress and peak strain, respectively, under a specific confinement and a loading rate and  $f'_c$  and  $\varepsilon_c$  are the peak stress and peak strain, respectively, with a same confinement but under static loading. In this paper, the slowest strain rate for each series is assumed as the static loading, that is, the static loading rate is between  $3.1\text{E-}5/\text{s}$  and  $4.8\text{E-}5/\text{s}$ . Strain rate sensitivities of  $D_f$  and  $D_s$  for all series are listed in Table 1. Figures 4 and 5 show the variation of  $D_f$  and  $D_s$  with respect to the strain rate. Average values for each strain rate are connected to each other if the points have a same yield strength ( $f'_y$ ), a same amount ( $\rho$ ) of confining spiral, and a same original concrete strength ( $f'_c$ ).

In Figure 4,  $D_f$  values are summarized for four combinations of  $\rho$  and  $f'_y$ . Figure 4(a) shows that  $D_f$  of unconfined concrete increases monotonically with increasing the strain rate. Monotonic increase of  $D_f$  with respect to the strain rate can be also seen for relatively low confinement of  $\rho=0.9\%$  in Figures 4(b) and (c) but the slope of lines are gentler. Specimens with high confinement ratio of  $\rho=2.0\%$  in Figure 4(d) do not show the monotonic increase very clearly and  $D_f$  rather seems constant for any strain rate.

In Figure 5,  $D_s$  values are summarized in a same manner as Figure 4.  $D_s$  for unconfined concrete in Figure 5(a) decreases with increasing strain rate up to strain rate of  $0.001/\text{s}$  or  $0.01/\text{s}$  and then increases afterward. Specimens with relatively low confinement of  $\rho=0.9\%$  in Figures 5(b) and (c) show that  $D_s$  decreases monotonically with increasing strain rate. It is noted that 54H1 Series in Figure 5(c) show the rebound of  $D_s$  at strain rate of  $0.01/\text{s}$  and this is similar to the unconfined concrete in Figure

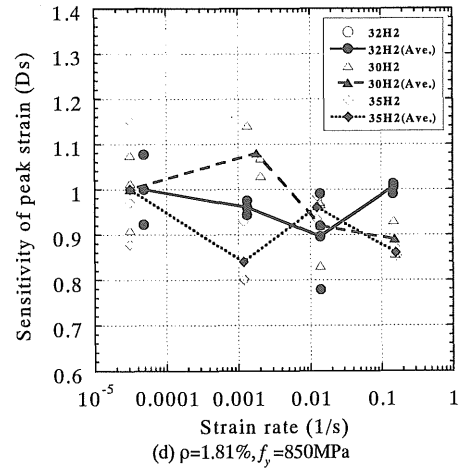
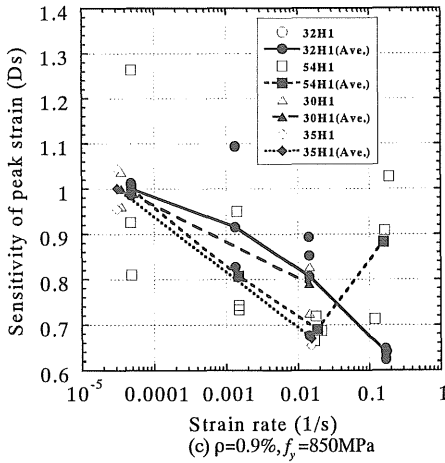
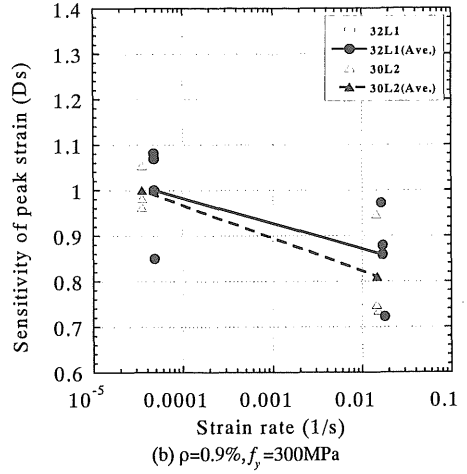
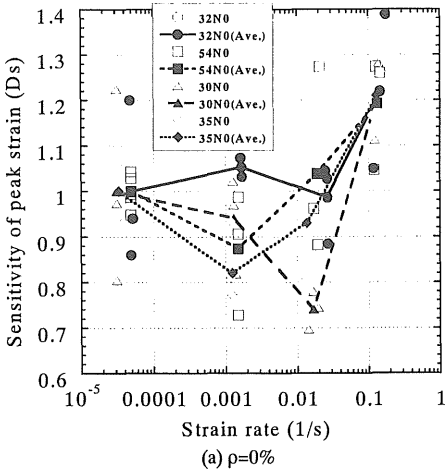


Figure 5. Strain rate sensitivity of peak strain,  $D_s$ .

5(a). Specimens with high confinement ratio of  $\rho=2.0\%$  in Figure 5(d) show very minor or negligible monotonic decrease with increasing strain rate.

From Figures 4 and 5, the variation of strain rate sensitivities of  $D_f$  and  $D_s$  is large for unconfined concrete but it becomes smaller or negligible as the confinement increases, and finally becomes negligible when the confinement increases up to  $\rho=1.81\%$  and  $f_y=850\text{MPa}$ .

### 3.4. Relation between the enhanced peak stress and the corresponding transverse stress

Figure 6 shows relations between enhanced peak stress and the corresponding transverse stress. Transverse stress,  $f_{rp}$ , was computed using Equation (3).

$$f_{rp} = \frac{\rho \cdot f_s}{2} \quad (3)$$

where  $\rho$  is the volume ratio of a spiral and  $f_s$  is the axial stress of the spiral at the peak. Value  $f_s$  was computed from the average axial strain of spirals measured at six or eight locations and its stress-strain relation. Each plot in Figure 6 has multiple points and a straight line. The line best fit the multiple points in each plot using the minimum lease square method. The equation representing the straight line is also shown at the bottom with a value of correlation factor,  $R$ . The correlation factors between 0.955 and 0.982 in Figure 6 are very high and the linear approximation is considered reasonable. The relation between the enhanced concrete strength and the transverse stress was first proposed by Richart et al. (1929) as Equation (4).

$$\frac{f'_{cc}}{f'_c} = 4.1 \frac{f_{rp}}{f'_c} + 1 \quad (4)$$

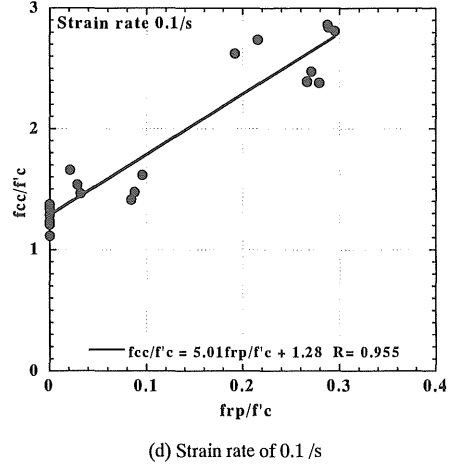
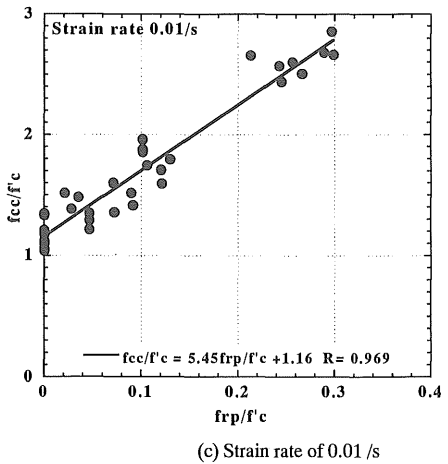
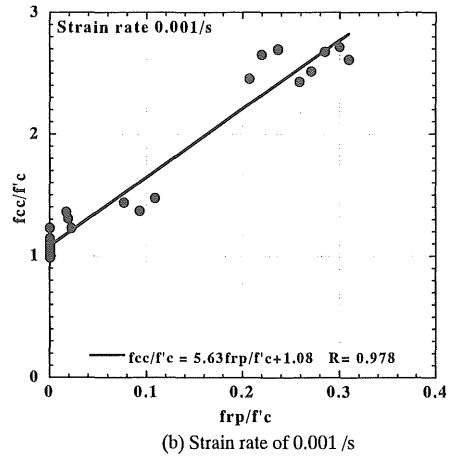
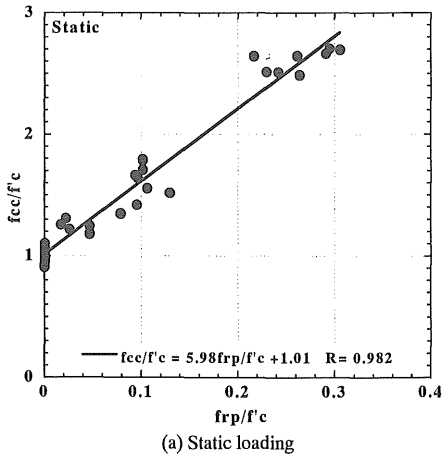


Figure 6. Relation between the peak stress,  $f'_{cc}$ , and confining stress,  $f'_p$ .

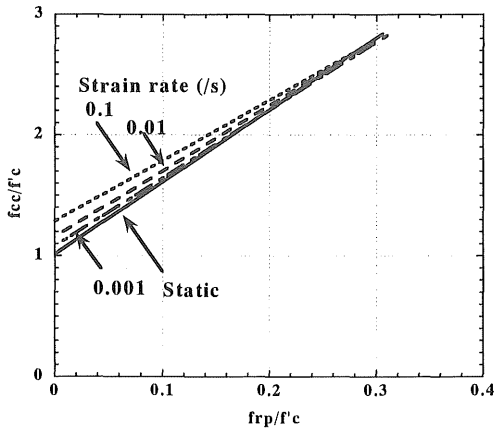


Figure 7. Strain rate sensitivity of the relation between the peak stress,  $f'_{cc}$ , and confining stress,  $f'_p$ .

Although the slopes in Figure 6 are different from 4.1 in Equation (4), the basic relation between the enhanced strength and the transverse stress still holds under dynamic loading. Four straight lines in Figure 6 are replotted in Figure 7. The figure shows that the enhanced concrete strength of the unconfined concrete under the strain rate of 0.1/s is 28 % larger than that under static loading. The four lines come close to each other as the transverse stress increases and finally intersect the line for static loading. The transverse stresses at the intersections are  $0.20f'_c$ ,  $0.28f'_c$ , and  $0.27f'_c$  for the strain rate of 0.001 /s, 0.01 /s, and 0.1, respectively. Although no experiment was carried out for the transverse stress greater than  $0.30f'_c$ , it is expected that all lines converge to the static line after the intersection. As a matter of fact, the observation in Figure 7 is the restatement of the increase in the peak stress due to the strain rate and the confining effects in Figure 4. However, the transverse stress expresses

more precisely the state of confinement rather than the amount and the yield strength of spirals.

#### 4. CONCLUSIONS

A total of one hundred twenty-six cylinder specimens was tested in order to study the strain rate effects on the compressive axial stress-strain relation of confined concrete. The strain rate ranged within the ordinary earthquake level and the confinement covered from no confinement to relatively high for ordinary civil and building structures.

Specimens showed two types of failure modes; concentric compression failure with vertical cracks or with a diagonal failure plane. Each failure mode was not specific to a certain combination of test variables.

The change of the shape of the dynamic stress-strain relation resulting from the confinement resembled that under static loading and the effect of strain rate on the shape was almost negligible. Hence, the prediction of the peak stress and peak strain will control the accuracy of the predicted stress-strain relations. The regression analysis on the relation between the enhanced peak stress and the transverse stress showed that the compressive strength of unconfined concrete increased about 30 % under the strain rate of 0.1 /s, and that this strength increase due to the strain rate decreased as the transverse stress increased and finally became zero when the transverse stress reached about 30 % of the original concrete strength.

The peak strain also had a strong strain rate sensitivity when the concrete was unconfined. This strain rate sensitivity of the peak strain decreased with increasing the strain rate but bounced back at strain rate between 0.001/s and 0.01/s. However, the difference in the strain rate sensitivity of the peak strain decreased with increasing the confining transverse stress similar to the trend of the peak stress.

#### ACKNOWLEDGMENTS

This research is a part of the project titled "Enhancement of Earthquake Performance of Infrastructures Based on Investigation Into Fracturing Process" supported by the Special Coordination Funds for Promoting Science and Technology (SCF) sponsored by the Science and Technology Agency (STA) in Japan. The contribution of the former students Mr. S. Horie, Mr. K. Fukuura, and Mr. N. Sugimoto to the experimental work is gratefully acknowledged.

#### REFERENCES

- Ahmad, S.H. & Shah, S.P. 1985. Behavior of Hoop Confined Concrete Under High Strain Rates. *ACI Journal*, Vol.82, No.5, Sep-Oct., 634-647.
- Dilger, W.H., Koch, R., & Kowalczyk, R. 1984. Ductility of Plain and Confined Concrete Under Different Strain Rates. *ACI Journal*, Vol.81, No.1, Jan-Feb., 73-81.

- Fafitis, A. & Shah, S.P. 1985. Lateral Reinforcement for High Strength Concrete Columns. *SP-87-12, ACI*, Detroit, 213-233.
- Mander, J.B., Priestley, M.J.N., & Park, R. 1988. Theoretical Stress-Strain Model for Confined Concrete. *Journal of Structural Engineering, ASCE*, Vol. 114, No. 8, August, 1804-1826.
- Mander, J.B., Priestley, M.J.N., & Park, R. 1988. Observed stress-strain behavior of confined concrete. *Journal of Structural Engineering, ASCE*, Vol. 114, No. 8, August, 1827-1849.
- Parakash, C., Desayi, Sundara Raja Iyengar. K.T. & Sanjeeva Reddy, T. 1978. Equation for Stress-Strain Curve of Concrete Confined in Circular Steel Spiral. *Materiau et Constructions*, Vol.11, No.65, Sept./October, 339-345.
- Park, R. & Leslie, P.D. 1977. Curvature Ductility of Circular Reinforced Concrete Columns Confined by the ACI Spirals. *6th Australian Conference on the Mechanics of Structures and Materials*, Vol.1, Technical Papers, Christchurch, New Zealand, August, 342-349.
- Richart, F.E., Brandzaeg, A. and Brown, R.L. 1929. The Failure of Plain and Spirally Reinforced Concrete in Compression. *University of Illinois Engineering Experimental Station, Bulletin No. 190*, 74 pp.
- Soroushian, P., Choi, K-B., & Alhamad, A. 1986. Dynamic Constitutive Behavior of Concrete. *ACI Journal*, Vol.83, No.2, Mar-Apr., 251-259.
- Soroushian, P. & Sim, J. 1986. Axial Behavior of Reinforced Concrete Columns under Dynamic Loads. *ACI Journal*, Vol.83, No.6, Nov-Dec., 1018-1025.
- Watanabe, F., Muguruma, H., Tanaka, H. & Katsuda, S. 1980. Improving the Flexural Ductility of Prestressed Concrete Beam by Using the High Yield Strength Lateral Hoop Reinforcement. *FIP Symposia on Partial Prestressing and Practical Construction in Reinforcement Concrete*, proceedings, Part 2, Sept., Bucuresti-Romania, 398-406.